

Spots on Am stars

L. A. Balona¹, G. Catanzaro², O. P. Abedigamba³, V. Ripepi⁴, B. Smalley⁵

¹South African Astronomical Observatory, P.O. Box 9, Observatory 7935, Cape Town, South Africa

²INAF-Osservatorio Astrofisico di Catania, Via S.Sofia 78, I-95123, Catania, Italy

³Department of Physics, North-West University, Private Bag X2046, Mmabatho, 2735, South Africa

⁴INAF-Osservatorio Astronomico di Capodimonte, Via Moiariello 16, I-80131, Napoli, Italy

⁵Astrophysics Group, Keele University, Keele, Staffordshire, ST5 5BG, UK

ABSTRACT

We investigate the light variations of 15 Am stars using four years of high-precision photometry from the *Kepler* spacecraft and an additional 14 Am stars from the K2 Campaign 0 field. We find that most of the Am stars in the *Kepler* field have light curves characteristic of rotational modulation due to star spots. Of the 29 Am stars observed, 12 are δ Scuti variables and one is a γ Doradus star. One star is an eclipsing binary and another was found to be a binary from time-delay measurements. Two Am stars show evidence for flares which are unlikely to be due to a cool companion. The fact that 10 out of 29 Am stars are rotational variables and that some may even flare strongly suggests that Am stars possess significant magnetic fields. This is contrary to the current understanding that the enhanced metallicity in these stars is due to diffusion in the absence of a magnetic field. The fact that so many stars are δ Scuti variables is also at odds with the prediction of diffusion theory. We suggest that a viable alternative is that the metal enhancement could arise from accretion.

Key words: stars: chemically peculiar – stars: oscillations – stars:variable

1 INTRODUCTION

The Am stars (metallic-lined A stars) are a group of A- and early F-type stars in which the CaII K line is relatively weak, and/or metallic lines relatively strong, compared with the spectral type indicated by the Balmer lines. More detailed analysis shows that Am stars are characterized by an under-abundance of Ca (and/or Sc) and/or an over-abundance of Fe and the Fe-group elements. The anomalous abundances in Am and Ap stars are thought to be a result of the interplay between gravitational settling and radiative acceleration of different atomic species. As a result, some elements diffuse upwards and others settle downwards provided there is little mixing. Mixing due to convection or meridional circulation due to rotation destroys the natural segregation of elements due to diffusion that would otherwise occur. Convection in A stars is confined to a very thin sub-surface layer which means that the diffusion process should proceed unhindered in slowly-rotating A stars.

The difference between Ap and Am stars is attributed to the fact that Ap stars have strong magnetic fields, whereas Am stars do not. Aurière et al. (2010) have confirmed that there is at least an order of magnitude difference in magnetic field strength between Ap/Bp stars and Am and HgMn stars. The presence of a large-scale strong dipole magnetic field in Ap stars modifies the diffusion rate in accordance

with the geometry of the field and is responsible for the abundance patches in Ap stars. On the other hand, the weak (or perhaps tangled) magnetic fields in Am stars leads to a relatively homogeneous abundance distribution across the stellar surface.

Early calculations predict a much larger over-abundance of heavy elements in Am stars than actually observed. Richer et al. (2000) found that it is important to consider the diffusion of heavy elements as well as helium. As the heavy elements settle, enrichment of the deeper iron bump opacity region of the iron-group causes a convective zone to develop in that region which mixes with the convective envelope by overshooting. The result is a dilution of the abundance anomalies, leading to abundances more in line with what is observed. More recent work shows that it is also important to include the destabilizing effect (thermohaline instability) caused by the composition gradient produced by diffusion (μ gradient) (Vauclair & Théado 2012).

It is thought that stars in binaries with orbital periods of 2–10 d become Am stars because their rotational velocities, v , have been reduced by tidal interactions below $v \approx 120 \text{ km s}^{-1}$, a requirement for diffusion to act. Both Am and normal stars occur in binaries with orbital periods between 10–100 d, but why this is the case is not understood. A recent search for eclipsing binaries among Am stars suggests that around 60–70 percent of Am stars are spectroscopic

binaries (Smalley et al. 2014), which is consistent with radial velocity studies (Abt & Levy 1985; Carquillat & Prieur 2007). Clearly, a substantial number of Am stars are probably single or in wide binaries and it is no longer clear whether binarity is a requirement for the Am phenomenon.

The effect of diffusion on pulsation of Am stars is to reduce the width of the instability strip, with the blue edge shifting towards the red edge, eventually leading to the disappearance of instability when helium is sufficiently depleted from the HeII ionization zone (Turcotte et al. 2000). The amount of driving is related to the amount of He still present in the driving zone. The cooler the star, the deeper the mixing and the greater the He abundance in the driving zone. Models therefore predict that Am stars should not pulsate unless they are sufficiently cool. More recent calculations suggest that rotational mixing is important in maintaining the He abundance in the driving region (Talon et al. 2006).

These ideas can be tested if we can obtain sufficiently accurate physical parameters to place pulsating and non-pulsating Am stars in the H-R diagram. Smalley et al. (2011) studied over 1600 Am stars and found that around 200 Am stars are pulsating δ Sct and γ Dor stars. It seems that Am stars, in general, seem to pulsate at somewhat lower amplitudes than normal δ Sct stars. However, Smalley et al. (2011) could find no real difference between the location of pulsating Am stars and δ Sct stars in the instability strip, except for a slight tendency of pulsating Am stars to be cooler than normal δ Sct stars. Catanzaro & Balona (2012) also concluded that there is a tendency for pulsating Am stars to be cooler than normal δ Sct stars and that the percentage of pulsating Am stars is about the same as the percentage of δ Sct stars in the instability strip. Similar conclusions were obtained by Balona et al. (2011c). It is clear that the prediction of diffusion theory regarding pulsation needs to be re-examined. The diffusion process, in fact, seems to play only a minor role in determining the pulsational stability of A and early F stars. Even Ap stars pulsate as δ Sct stars at low amplitudes (Balona et al. 2011a).

Recent high-precision photometric observations of A stars using *Kepler* have further undermined the general consensus that these stars have stable envelopes where diffusion has a strong competitive advantage. It seems that about 2 percent of A stars observed by *Kepler* show flares (Balona 2012, 2014c). It can be easily demonstrated that the flares are associated with the A star and not with a presumed cool companion. Furthermore, the *Kepler* data suggest that at least 40 percent of A stars are rotational variables (Balona 2013), presumably due to starspots. Since it is generally believed that Am stars do not have magnetic fields, the incidence of rotational modulation should be absent or small in Am stars compared to normal A stars.

The previous study of *Kepler* Am stars (Balona et al. 2011c) used only data for approximately the first 50 d and was mainly aimed at detecting δ Sct pulsations in these stars. The low-amplitude light variations due to rotational modulation were suspected but could not be studied. There are now four years of almost continuous high-precision photometry for these stars, making it easier to detect rotational modulation. In this paper we investigate rotational modulation in Am stars using *Kepler* data. Our aim is to establish whether the incidence of rotational modulation or other activity is lower in Am stars than in normal A stars. The

answer might explain why there are many slowly-rotating A stars which are not Am stars and provide further clues as to the nature of the Am phenomenon.

2 THE DATA

There are 15 known Am stars in the *Kepler* field (Balona et al. 2011c). We also include 14 Am stars observed by the *Kepler* K2 Campaign 0 mission. These data are far less favourable to detecting rotational modulation because only about 45 d of data are available and the photometric precision is severely compromised by the telescope motion. However, The K2 data are useful in detecting δ Sct pulsations in these stars.

For the vast majority of stars, *Kepler* photometry is available only in long-cadence (LC) mode which consist of practically uninterrupted 30-min exposures covering a time span of over three years. For a few thousand stars, including all the Am stars discussed here, short-cadence (SC) 1-min exposures are also available, but these usually cover only one or two months. Characteristics of LC data are described in Jenkins et al. (2010b) while Gilliland et al. (2010) describe the characteristics of SC data. The science processing pipeline is described by Jenkins et al. (2010a). The *Kepler* data are divided into quarters of approximately 90-d duration which are numbered Q0, Q1, Q2, etc., Q0 being the initial 10-d commissioning run. In this study we use all available LC data (Q0 – Q17) from JD 2454953 to JD 2456424 (1471 d). These data are publicly available on the Barbara A. Mikulski Archive for Space Telescopes (MAST, archive.stsci.edu).

The light curve files contain simple aperture photometry (SAP) values and a more processed version of SAP with artifact mitigation included called Pre-search Data Conditioning (PDC) flux. The SAP photometry contains discontinuities, outliers, systematic trends and other instrumental signatures. The PDC tries to remove these errors while preserving astrophysically interesting signals by using a subset of highly correlated and quiet stars to generate a cotrending basis vector set. The PDC flux uses the best fit that simultaneously removes systematic effects while reducing the signal distortion and noise injection. Details of how this is accomplished are described in Stumpe et al. (2012) and Smith et al. (2012). Because we are interested in low-frequency variations, we have used the PDC fluxes in this analysis.

The *Kepler* SAP data contains drifts and jumps. There is a zero-point difference between data in different quarters and the instrumental drift varies from quarter to quarter. Although the PDC data are designed to remove these effects, it is possible that residual long-term instrumental effects are still present at a low level. To understand how correction of data may effect the low-frequency end of the periodogram, we performed a simple simulation where we applied our own correction to the SAP data of a few stars which appeared to be the least variable among 20000 *Kepler* stars. To correct the SAP data we fitted and removed polynomials of low degree (typically degree 3 or 5) to individual quarters. The polynomials do not join smoothly between any two quarters, but we ignored these small jumps. To these data we added sinusoidal variations comprising of 100 frequencies

of equal amplitudes and random phases. These frequencies start at zero frequency and are equally spaced by 0.1 d^{-1} . The periodogram recovers all frequencies, including the lowest frequency of 0.1 d^{-1} . The same simulation using a signal of 0.02 d^{-1} recovers a lowest frequency of 0.08 d^{-1} . From this simulation, we may deduce that frequencies higher than about 0.08 d^{-1} are not affected by the crude correction procedure. The corrections used to obtain the PDC data are, of course, more sophisticated and we can safely assume that frequencies higher than 0.08 d^{-1} are easily recovered.

The light curves from the extended *Kepler* K2 Campaign 0 mission were obtained from the raw pixel data files using a suitable aperture. Our own software, *keplc*, was used for this purpose. For fields where there were few or faint stars in close proximity to the target, we used the largest possible aperture in order to minimize the instrumental light variation due to image motion. The telescope motion can be found by tracking the centroid of the star. There is a 4.08 d^{-1} periodic component in the image motion which is reflected in the light curve. We therefore removed this frequency and all its harmonics from the light curve so as to enhance the actual stellar signal. Long-term drifts and jumps were also removed. The periodogram of the processed light curve was then calculated. Due to image motion and long-term drifts, the periodogram noise level for the K2 data increases strongly towards zero frequency. As a result, it is generally not possible to detect low frequencies in the star unless these are of high amplitude.

3 KEPLER LIGHT CURVES

A list of known Am stars in the *Kepler* and K2 Campaign 0 fields is shown in Table 1. The identifications are from the *Kepler* Input Catalogue (KIC, Brown et al. (2011)) and from the K2 Ecliptic Plane Input Catalog (EPIC, <https://archive.stsci.edu/k2/KSCI-19082-002.pdf>). The spectral classification for Am stars in the *Kepler* field are mostly quite recent and detailed metal abundances are available for most of the stars. The Am nature of these stars is hardly in doubt. The spectral classification for Am stars in the K2 field are far less secure. All of them are listed as Am stars by Renson & Manfroid (2009), but the original reference is often missing. In Table 1 we have referenced what we believe to be the original source, but sometimes the Am nature is not even mentioned. Part of the problem may be in the way the recognition of the Am class has evolved with time.

Examination of the light curves shows that of the 29 Am stars, there are 12 δ Sct variables, 1 γ Dor variable and 2 detached eclipsing binaries. Most of the others have light curves similar to those generally attributed to rotational modulation caused by starspots. Periodograms of the δ Sct Am stars in the *Kepler* field are shown in Fig. 1. Periodograms of the other stars in the *Kepler* field are shown in Fig. 2.

It is evident from Fig. 2 that highly significant, coherent, low-frequency variations and harmonics are present in all six non- δ Sct stars. In KIC 3836439 this can be attributed to proximity effects in a binary. Luyten (1936) found the star to be a spectroscopic binary with $P_{\text{orb}} = 1.54039 \text{ d}$, semi-amplitude $K = 88.7 \pm 2.8 \text{ km s}^{-1}$ and a circular orbit. Batten et al. (1978) further lists the mass function

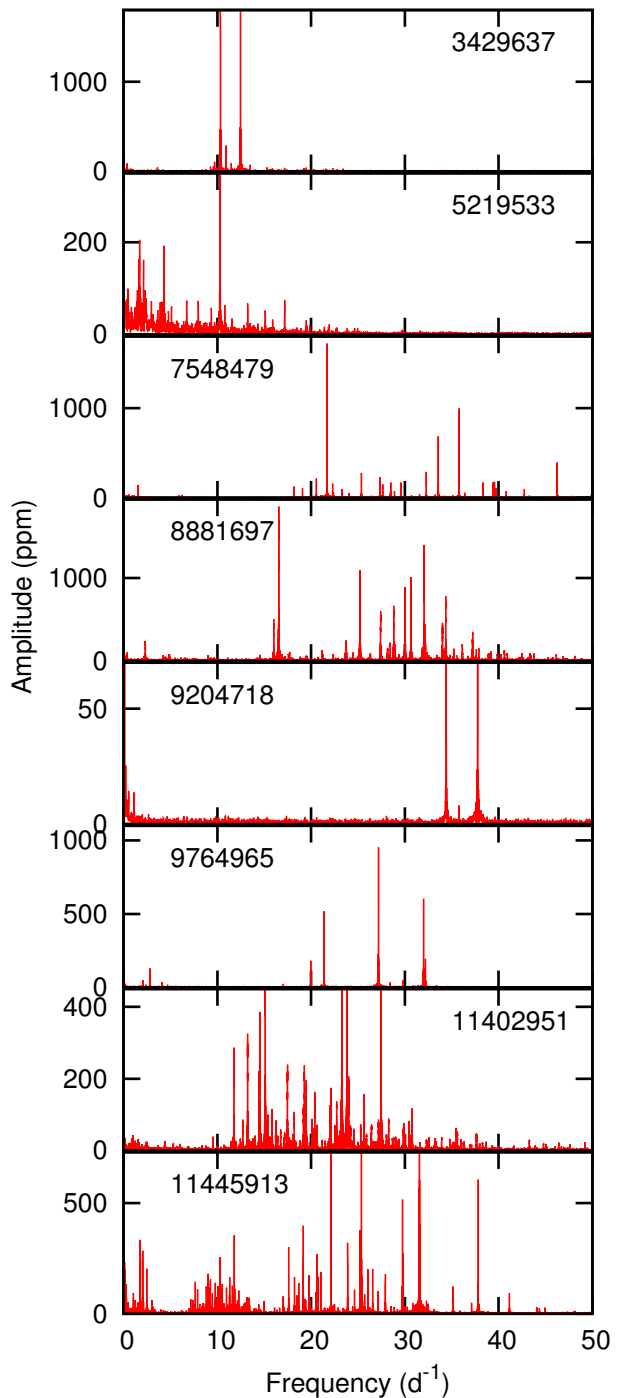


Figure 1. Periodograms of short-cadence light curves of Am stars in the *Kepler* field which are δ Scuti variables.

$f(m) = 0.112$ and $a_1 = 1.88 \times 10^6 \text{ km} = 2.68R_{\odot}$. *Kepler* observations confirm that this is an eclipsing binary with $P = 1.540407 \text{ d}$ in a detached Algol-type system with $\sin i = 0.96$ (Slawson et al. 2011). The ratio of effective temperatures $T_2/T_1 = 0.758$ and the sum of radii $R_1 + R_2 = 0.35a$ where a is the semi-major axis. Slightly different results are given by Prša et al. (2011): $\sin i = 0.95$, $T_2/T_1 = 0.48$ and $R_1 + R_2 = 0.37a$. It is possible that the Am classification is a result of a composite spectrum.

Table 1. List of Am stars in the *Kepler* field (top) and the K2 Campaign 0 field (bottom). The stars are identified by their KIC number and their EPIC number respectively while the second column is the HD number. The spectral classification is given in the third column. The apparent magnitude and the derived effective temperature, T_{eff} , are mostly from the KIC except where noted. The surface gravity, $\log g$ and projected rotation velocity, $v \sin i$, are from Uytterhoeven et al. (2011) except where noted. The variable star classification is estimated from the light curve and periodogram. The rotation period of the star (P_{rot} in days) and the rotational light amplitude (A in ppm) is estimated from the periodogram. References are as follows: 1 - Abt (1981), 2 - Abt (1984), 3 - Ammons et al. (2006), 4 - Antoci et al. (2011), 5 - Bertaud (1960), 6 - Catanzaro et al. (2011), 7 - Catanzaro & Ripepi (2014), 8 - Catanzaro et al. (2015), 9 - Floquet (1970), 10 - Floquet (1975), 11 - (Halbedel 1985), 12 - McCuskey (1967), 13 - McCuskey (1959), 14 - Renson & Manfroid (2009).

KIC/EPIC	HD	Sp. Type	V	T_{eff} (K)	$\log g$ (dex)	$v \sin i$ (km s^{-1})	Type	P_{rot} (d)	A (ppm)
3429637	178875	kF2hA9mF3 ²	7.71	7100 ⁶	4.00	50	DSCT		
3836439	178661	kA2.5hF0mF0 ¹	7.57	7166	3.90		EA		
5219533	226766	kA2hA8mAs ²	9.20	7409	3.90	115	DSCT		
7548479	187547	A4Vm ⁴	8.40	7500 ⁴	3.90	10	DSCT/ROT	0.6530	150
8323104	188911	A2mF0 ¹⁰	9.66	7587	3.90		ROT	6.0447	7
8703413	187254	A2mF0 ¹⁰	8.71	7960 ⁷	3.80 ⁷	15 ⁷	ROT	6.5292	215
8881697		A5m ⁵	10.57	7732	3.90		DSCT/ROT	0.4319	200
9117875	190165	A2mF2 ¹⁰	7.51	7460 ⁷	3.60 ⁷	58 ⁷	ROT	1.4949	42
9204718	176843	A3mF0 ¹⁰	8.79	7610 ⁷	3.80 ⁷	27 ⁷	DSCT/ROT	8.7308	90
9272082	179458	A5m ⁹	9.00	8150 ⁷	3.90 ⁷	75 ⁷	ROT	0.9703	4
9349245	185658	Am: ⁸	8.15	8300 ⁸	4.00 ⁸	80 ⁸	ROT	0.9420	7
9764965	181206	Am: ⁸	8.85	7800 ⁸	3.88 ⁸	87 ⁸	DSCT/ROT	0.4872	135
11402951	183489	kF3hA9mF5 ²	8.13	7150 ⁶	3.50	100	DSCT		
11445913	178327	kA7hA9mF5 ²	8.49	7200 ⁶	3.50	51	DSCT		
12253106	180347	Am ⁸	8.41	7900 ⁸	3.85 ⁸	12 ⁸	ROT	4.1043	82
202059291	40788	A2 ¹² , A2m ¹⁴	9.04	7576 ³			SB2	2.984	188
202059336	43509	Am ⁸	8.90	7900 ⁸	3.97 ⁸	28 ⁸			
202061329	250408	A2 ¹² , A2m ¹⁴	10.36	8329 ³					
202061333	250786	A7 ¹² , A5m ¹⁴	10.40	7431 ³			DSCT		
202061336	251071	F0V ¹² , A3m ¹⁴	10.34	7316 ³					
202061338	251150	A2 ¹² , A0m ¹⁴	10.57	7959 ³			DSCT		
202061349	251947	A3p: ¹² , A2m ¹⁴	10.95	6561 ³					
202061353	252154	F2V ¹² , A5m ¹⁴	9.85	6925 ³			DSCT		
202061363		A0m: ¹³	11.00	4569 ³					
202062436		A2-F0 ¹²	11.64	6500			DSCT		
202062447	251717	A3-F2 ¹²	11.20	7396 ³			GDOR		
202062450	256320B	kA5hA8mF5 ¹¹	10.80						
202062454	251812	A5-F2: ¹²	11.61	6750 ³					
202062455	251463	A5-F2 ¹²	10.70	6220 ³					

In the other stars, the low-frequency variations are unlikely to be due to proximity effects in a binary because the amplitudes often vary and the periodogram lines attributed to rotation are broadened in some stars. This is to be expected in a rotational variable because spots change in size and intensity with time. Differential rotation, which appears to be a general feature in A stars (Balona 2013), will also cause such broadening. As an example of rotational modulation, Fig. 3 shows part of the long-cadence PDC light curve of KIC 8323104. Quasi-regular light variability is present with a peak-to-peak amplitude of about 40 ppm and a timescale of around 6 d. This cannot be a result of proximity effects in a binary because of the irregularity of the variations. The most plausible explanation is that it is a result of rotational modulation due to stellar activity.

The second-last column of Table 1 shows the rotation period estimated from the periodogram. In the case of δ Sct stars there are often many other low-frequency peaks which are always present in any δ Sct star. In this case we identified the rotation peak because of its relatively high ampli-

tude and the presence of an harmonic (Balona 2013). The presumed rotation period decreases with $v \sin i$, as might be expected.

KIC 8703413 was first reported as an Am star by Mendoza (1974) and subsequently classified as kA2mF0 by Floquet (1975). The star was confirmed as Am by Catanzaro & Ripepi (2014). As can be seen in Fig. 4, the *Kepler* light curve shows distinct beating and traveling wave characteristic of star spots (Uytterhoeven et al. 2011; Balona 2013). The periodogram shown in the middle panel has a main peak at $f_1 = 0.1532 \text{ d}^{-1}$ and its harmonics. In addition, there is another peak $f_2 = 0.1404 \text{ d}^{-1}$ which looks to be a bit broader. It is not clear how this pattern may be interpreted, but it seems reasonable to suppose that either f_1 or f_2 could be the rotation frequency. Perhaps both frequencies could be ascribed to starspots if the star is in differential rotation. No other frequencies are present. The projected rotational velocity, $v \sin i = 15 \pm 2 \text{ km s}^{-1}$, is compatible with the rotation frequency, giving a radius $R \sin i \approx 1.96 R_{\odot}$. There are seven radial velocities in the literature (Fehrenbach et al. 1997), which is not enough for an

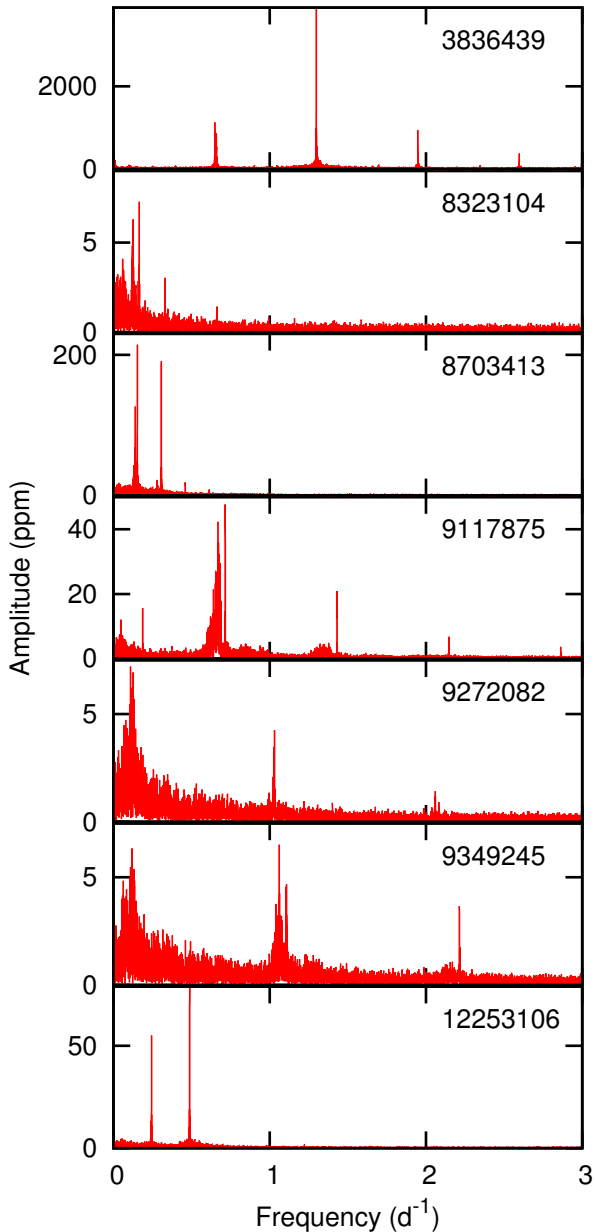


Figure 2. Periodograms of long-cadence light curves of Am stars in the *Kepler* field which are not δ Sct variables.

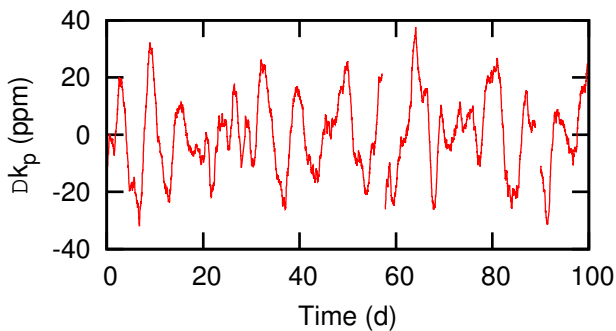


Figure 3. Portion of the corrected *Kepler* light curve of KIC 8323104 showing regular variations.

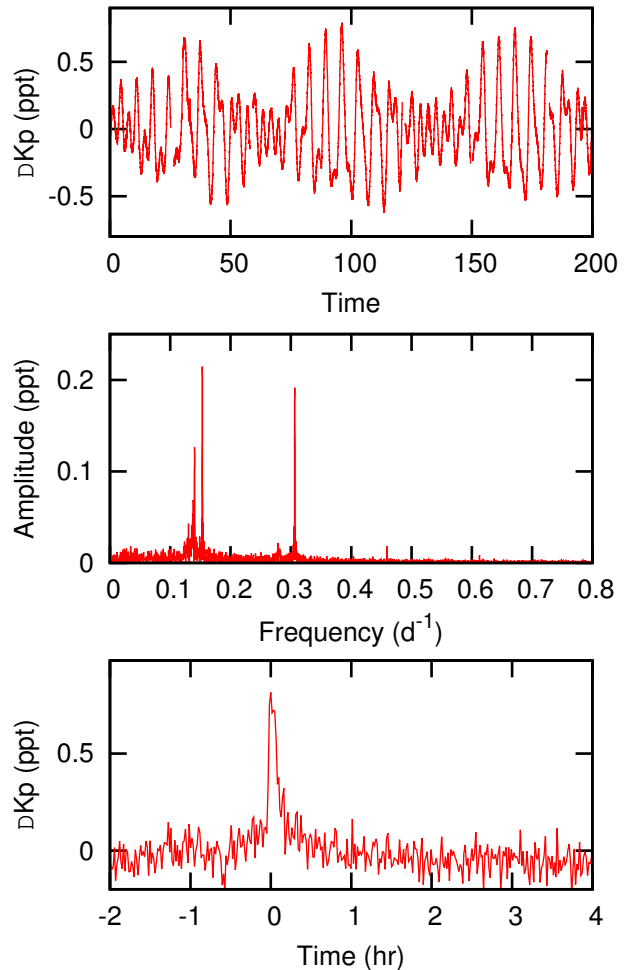


Figure 4. Top panel: part of the *Kepler* long-cadence light curve of KIC 8703413 showing traveling features typical of starspots. Middle pane: periodogram of all LC data. Bottom panel: presumed flare at JD 2455164.88 seen in SC data.

analysis. The velocity range is quite large and it is possible that the star may be a binary.

KIC 8703413 is a flare star (Balona 2012) as can be seen in the bottom panel of Fig. 4. The flare intensity is about 0.7 ppt. The A star has a luminosity of about 100 times larger than a K dwarf, which means that if the flare is attributed to an unseen K dwarf companion, its relative intensity would have to be about 70 ppt. The mean flare intensities in *Kepler* field K-dwarfs are about 3.3 ppt (Walkowicz et al. 2011), which means that this particular flare would have to be of unusual intensity. In general, flares in A stars cannot be attributed to a cool companion since the average flare intensity is about two orders of magnitude larger than that in a typical K or M dwarf.

For KIC 3429637, Catanzaro et al. (2011) obtained $T_{\text{eff}} = 7300 \pm 200$ K, $\log g = 3.16 \pm 0.25$ and $v \sin i = 50 \pm 5$ km s $^{-1}$, values later confirmed by Murphy et al. (2012). The remarkable amplitude increase in the δ Sct pulsations of this star has been discussed by Murphy et al. (2012). Since that time, additional *Kepler* data show a more complex amplitude variation for the frequencies of largest amplitude (Fig. 5, top panel). While $f_1 = 10.337$ d $^{-1}$ and

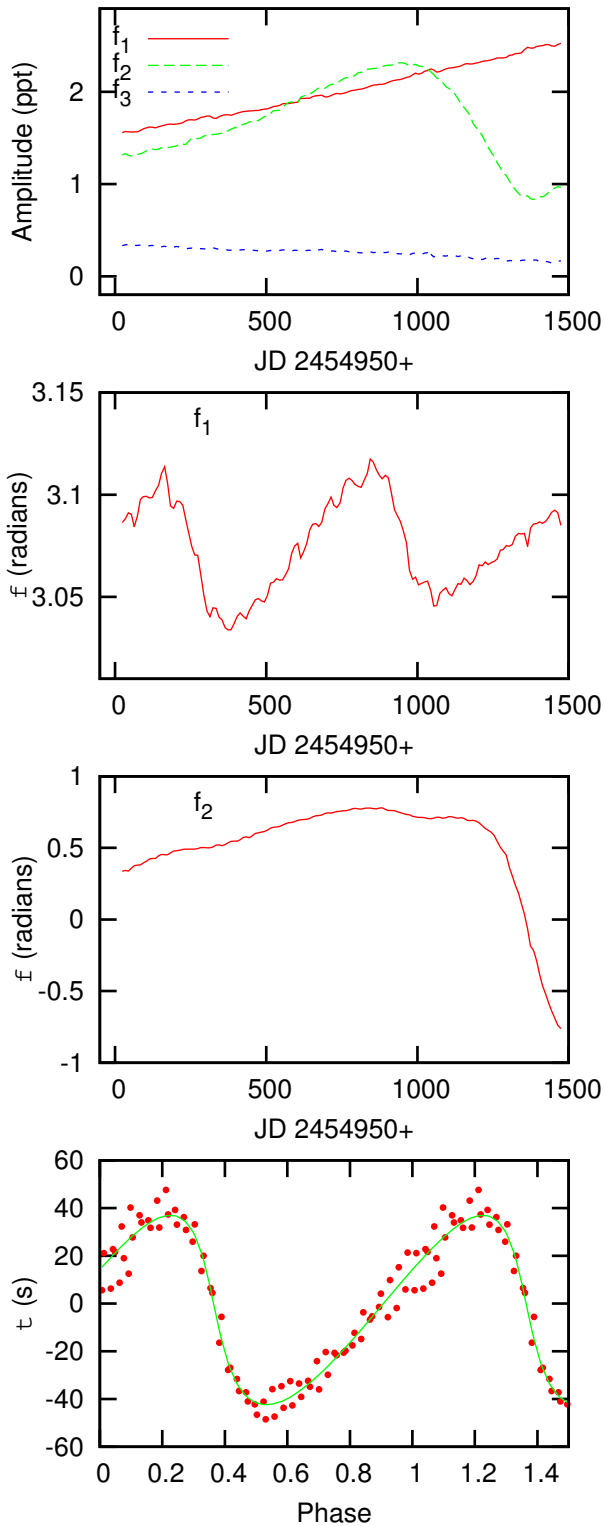


Figure 5. Top panel: amplitude variation of the three highest amplitude pulsation modes in KIC 3429637 from *Kepler* photometry. The next panels from the top shows the phase variation of f_1 and f_2 . In the bottom panel the time delay variation, τ , derived from f_1 and f_2 are phased with the orbital period of 704.7 d. The solid line is from the orbital solution. The time of phase zero is JD 2454950.0.

$f_3 = 10.936 \text{ d}^{-1}$ show steady amplitude changes, the steady amplitude increase for $f_2 = 12.472 \text{ d}^{-1}$ reverses and decreases sharply around JD 2455950. The latest observations indicate that the amplitude of f_2 is, once again, increasing. The timescale seems to be too short for an evolutionary explanation, as suggested by Murphy et al. (2012).

KIC 5219533 has a very rich δ Sct frequency spectrum, including a large number of modes in the γ Dor range. The projected rotational velocity is $v \sin i = 115 \text{ km s}^{-1}$. The principal peak at $f_1 = 10.2853 \text{ d}^{-1}$ is clearly variable in frequency. The phase, ϕ , varies smoothly in the range $2.0 < \phi < 4.0$ radians over 400 d which corresponds to approximately 0.0008 d^{-1} .

A recent abundance analysis of KIC 9117875 by Catanzaro & Ripepi (2014) indicates $T_{\text{eff}} = 7400 \pm 150 \text{ K}$, $\log g = 3.6 \pm 0.1 \text{ dex}$, and $v \sin i = 58 \pm 6 \text{ km s}^{-1}$. Both Ca and Sc show underabundances of about 1 dex, while the heavy elements are all overabundant: 0.5 dex for iron-peak elements and about 2 dex for Ba. The Am nature of this star is thus confirmed. The *Kepler* light curve shows beating and low frequencies resembling a γ Dor star and it was classified as such by Uytterhoeven et al. (2011). However, a more detailed examination of the periodogram shows a broad feature at about $f_1 = 0.672 \text{ d}^{-1}$ with a very sharp neighbouring peak at $f_2 = 0.7157 \text{ d}^{-1}$. Several harmonics of f_2 are visible, which is quite unlike the structure found in typical γ Dor stars. In fact, this mysterious structure is found in a considerable fraction of A stars, but is unexplained (Balona 2013). Balona (2014c) suggests that the sharp feature might be explained by a synchronously orbiting planet, not necessarily transiting. Assuming that f_1 is the rotation frequency and using the above projected rotational velocity leads to a radius $R \sin i \approx 1.69 R_{\odot}$, which is reasonable for an A star.

There is a further mystery regarding this star in that it appears to flare. In Fig. 7 we show examples of possible flares in this star in the *Kepler* LC data. It should be noted that LC data is not ideal to detect flares since the exposure time of 30 min is a considerable fraction of the duration of the flare. Short-cadence data are available for this star, but only for about 10 d during Q0.

KIC 9204718 was confirmed as an Am star by Catanzaro & Ripepi (2014) who find $T_{\text{eff}} = 7600 \pm 150 \text{ K}$, $\log g = 3.8 \pm 0.1 \text{ dex}$ and $v \sin i = 27 \pm 3 \text{ km s}^{-1}$. There are clearly several low-frequency peaks in the periodogram, as shown in Fig. 8. The largest peak is at 0.1145 d^{-1} and its harmonic. These peaks are both rather broad suggesting amplitude or frequency modulation; in fact, the light variation with this frequency is clearly visible in the light curve (Fig. 8). This variation is suggestive of a starspot, in which case 0.1145 d^{-1} would be the rotation frequency. This is reasonable since we measured $v \sin i = 27 \pm 3 \text{ km s}^{-1}$.

Even more interesting is the presence of several harmonics of 0.5474 d^{-1} . If we remove the 0.1145 d^{-1} and the δ Sct frequencies from the data, what is left is the 0.5474 d^{-1} variation and its harmonics. By binning the light curve and averaging the data in each bin, we obtained the phased light curve shown in the bottom panel of Fig. 8. There is no simple explanation for this variation. It cannot be the rotational frequency, since this has already been identified. The light curve resembles that of a contact binary, but if so it implies that the rotational period is not synchronized with the orbital period.

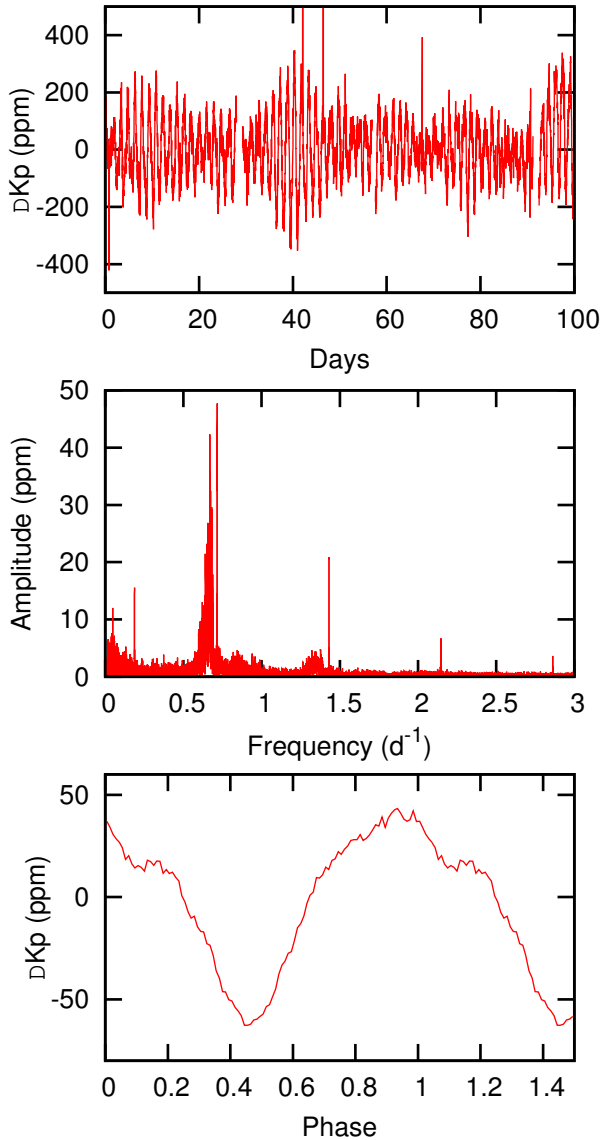


Figure 6. Top panel: part of the *Kepler* long-cadence light curve of KIC 9117875. The middle panel is the periodogram showing the broad feature, f_1 and the sharp peak f_2 and its many harmonics. The bottom panel shows the light curve when all frequencies except for f_2 and its harmonics have been removed. The data points have been averaged for clarity.

There is a great deal of uncertainty regarding the nature of KIC 9272082. Macrae (1952) noted its possible peculiar spectrum, but did not give any details. Bertaud (1960) gives a classification of A5m, but Floquet (1970) classified it as a normal A7 star. The star is included as an Am star in the Renson & Manfroid (2009) catalogue. Catanzaro & Ripepi (2014) found it to be an A4 main sequence star with $T_{\text{eff}} = 8500 \pm 200$ K, $\log g = 3.9 \pm 0.1$ dex and $v \sin i = 75 \pm 7$ km s $^{-1}$. Most of the elements in this star are somewhat overabundant by about 0.5–1.8 dex. However, Si, Cr, Ni, and Ba have normal abundances. Although the abundance pattern is not typical, it does not conform to that expected for Am stars.

The light curve (top panel of Fig. 9) shows distinct variations which are confirmed by the periodogram (middle

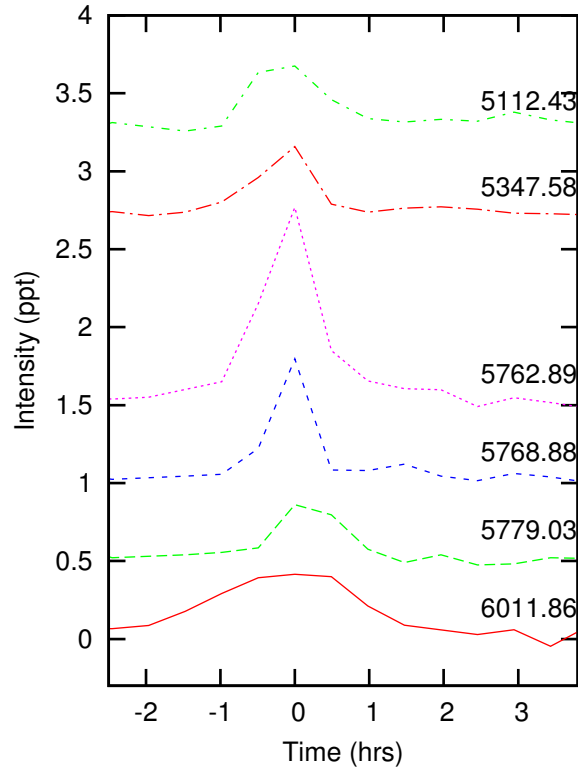


Figure 7. Possible flares in LC data of KIC 9117875. The labels give the JD of peak flare intensity relative to JD 2450000.00.

panel). There is a constant frequency $f_1 = 1.03058$ d $^{-1}$ and its harmonic, suggestive of rotational modulation. The corrected LC data phased with this frequency shows a roughly sinusoidal variation (Fig. 9), which we assume to be rotational modulation.

4 BINARY MOTION FROM TIME DELAY

It is generally thought that most Am stars are binaries with orbital periods in the range 1–10 d (Abt 1967). It is of interest to determine whether any of the stars in our sample are spectroscopic binaries. A pulsating star in a binary system acts as a clock. If the star is a member of a binary system, its distance will vary as it orbits the barycentre. The changing distance leads to a variable phase of pulsation. The method has been discussed by Shibahashi & Kurtz (2012) using data transformed to the frequency domain. More recently, Murphy et al. (2014) has used the more direct analysis of phase variation. Application to δ Sct stars is difficult because of the many close frequencies which distort the phase variation. By direct minimization of the photometric error, it is possible to construct a diagram similar to the periodogram where the orbital semi-major axis is shown as a function of the orbital period (the binarogram). This technique allows relatively quick detection of binary candidates (Balona 2014a).

KIC 3429637 has been discussed above in the context of its δ Sct pulsations. Fig. 5 also shows the phase variations of f_1 and f_2 . We used a window with semi-width of 20 d and a sampling interval of 20 d. The dominant frequency,

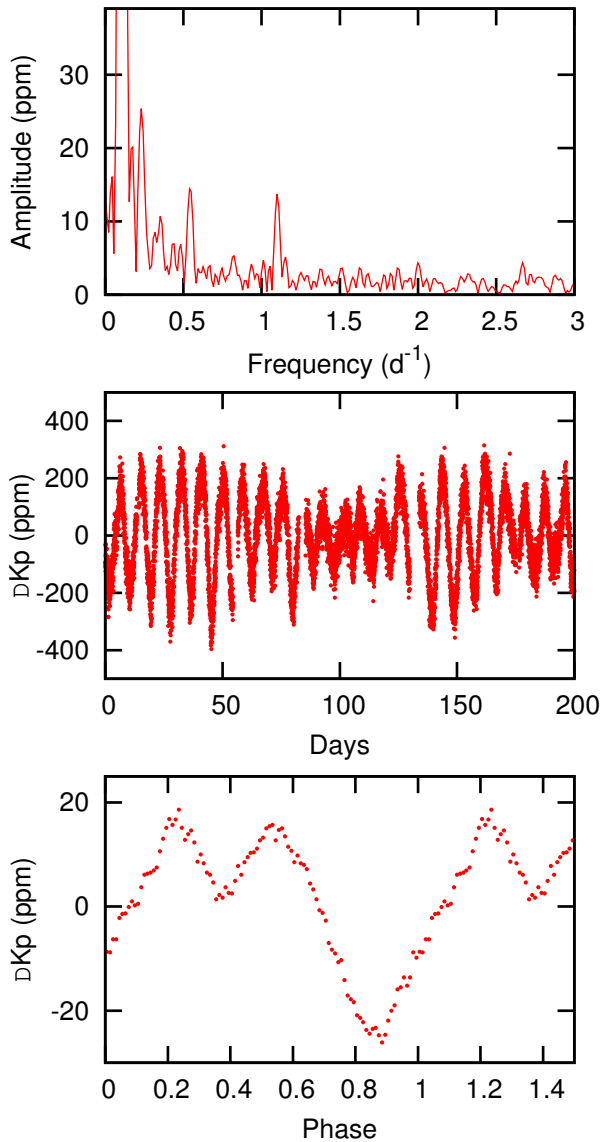


Figure 8. Top panel: periodogram of KIC 9204718 showing several low frequencies. Middle panel: part of the light curve showing the dominant 0.1145 d^{-1} frequency. Bottom panel: phased and averaged light curve showing the 0.5474 d^{-1} light variation.

f_1 , shows a clear periodic variation with $P = 704.7 \text{ d}$. There is a rather sudden change in phase of f_2 (corresponding to a change in frequency) at a time soon after the sharp decrease in amplitude shown in the top panel. Close inspection reveals that the 704.7-d period is also present in the phase variation of f_2 . Short-cadence observations are available for this star, so there is no ambiguity regarding the frequencies.

We applied the time-delay algorithm described above to both f_1 and f_2 . Because there is a strong sudden decrease of amplitude and frequency around JD 2455950, we decided to use only the data up to this date. There is still a long-term trend which was removed by fitting a Fourier series combined with a polynomial of third degree. The derived time delay variation for f_1 and f_2 are in good agreement and both are shown in the bottom panel of Fig. 5 phased with the orbital period. By fitting the time delay variation

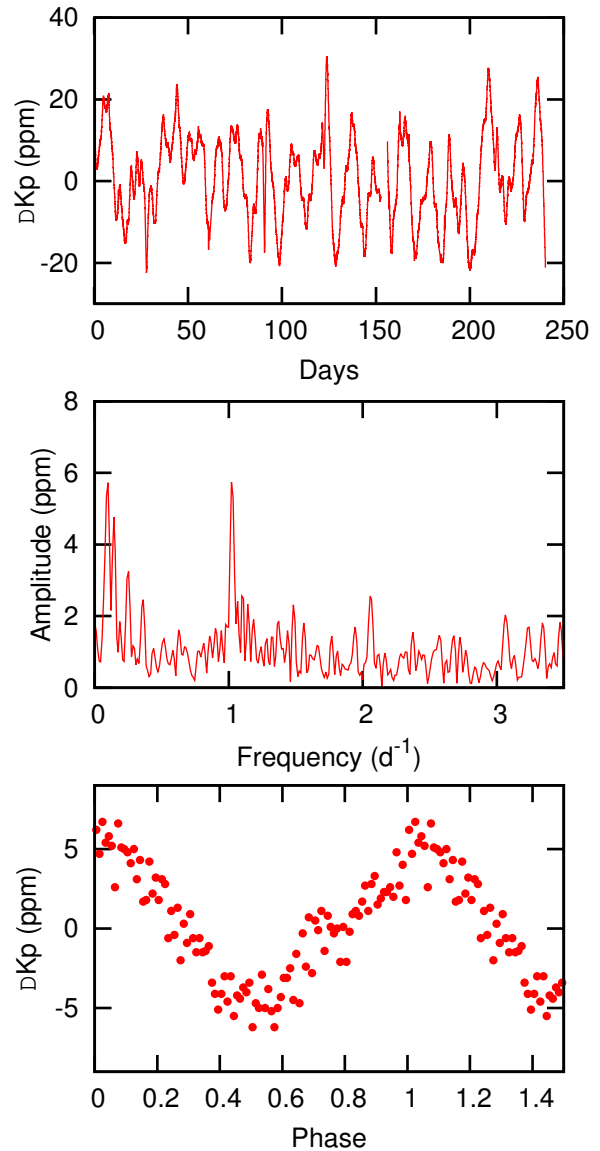


Figure 9. Top panel: portion of the corrected *Kepler* light curve of KIC 9272082. The light curve has been smoothed by a Gaussian filter with FWHM = 0.5 d for better visibility. Middle panel: periodogram of the LC data. Bottom panel: binned light curve phased with frequency $f_1 = 1.03058 \text{ d}^{-1}$.

we obtain the orbital solution shown in Table 4 and shown in the bottom panel of Fig. 5.

For KIC 11445913 short cadence observations show that the dominant peaks are at $f_1 = 31.5578$, $f_2 = 25.3771$, $f_3 = 22.1330$ and $f_4 = 37.8204 \text{ d}^{-1}$. As usual there are quite a number of low-frequency peaks, but none that could be identified as due to starspots. The value $v \sin i = 51 \pm 1 \text{ km s}^{-1}$ (Balona et al. 2011c). Time delay analysis of f_1 , f_2 and f_3 shows that they have the same phase variation, but the period, if it exists, is considerably longer than the almost 4 yr duration of the *Kepler* data. Fig. 10 shows the resulting radial velocities derived from the first derivative of the time delay variation. This star might be a binary with a period of around 10 yr or longer.

Table 2. Binary elements of KIC 3429637 from the time delay of the *Kepler* light curve. The orbital period P_{orb} , half-range of primary radial velocity variation K_1 , eccentricity e , longitude of periastron ω , JD of periastron T_{per} , projected semi-major axis of the primary $a_1 \sin i$, and mass function $f(M)$.

Parameter	Value	Units
P_{orb}	704.7 ± 4.4	days
K_1	1.79 ± 0.08	km s^{-1}
e	0.61 ± 0.04	
ω	3.05 ± 0.02	radians
T_{per}	2455204.6 ± 3.6	
$a_1 \sin i$	0.100 ± 0.005	AU
$f(M)$	$(2.69 \pm 0.03) \times 10^{-4}$	M_{\odot}

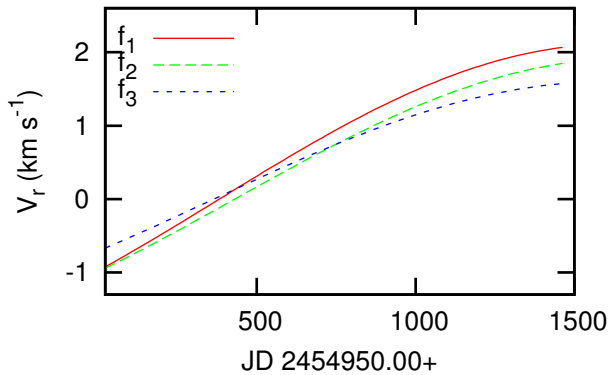


Figure 10. Radial velocity curves derived from frequencies f_1 , f_2 and f_3 in KIC 11445913.

5 K2 LIGHT CURVES

Owing to the failure of two of the four reaction wheels, the *Kepler* spacecraft has lost its pointing ability. The telescope drift is corrected at regular intervals, with the result that there is substantial image drift and a large increase in photometric error from about 20 ppm for the original *Kepler* field to about 300 ppm for the K2 field. Here we present results for Am stars observed in the first K2 scientific mission, Campaign 0. The observations occur over a timespan of about 77 d, but with a large gap of 26.5 d. The total on-target time is about 47 d. This rather short time and the much increased scatter severely compromises detection of significant frequencies less than about 3 d^{-1} .

Many of these stars were observed by the *STEREO* spacecraft. No significant variability could be found for EPIC 202059291, 202059336, 202061329, 202061333, 202061336, 202061338 and 202061363 from *STEREO* observations Paunzen et al. (2013). The remarkably low effective temperature for EPIC 202061363 reported in Ammons et al. (2006) is confirmed by our own analysis of available multicolour photometry. *STEREO* observations of EPIC 202061349 also do not show any significant variability (Wraight et al. 2012). Of these stars, we detected variability in EPIC 202059291, 202061333 and EPIC 202061338 (see below). Some of the stars are δ Sct variables. The periodograms of the δ Sct stars are shown in Fig. 11. The effective tem-

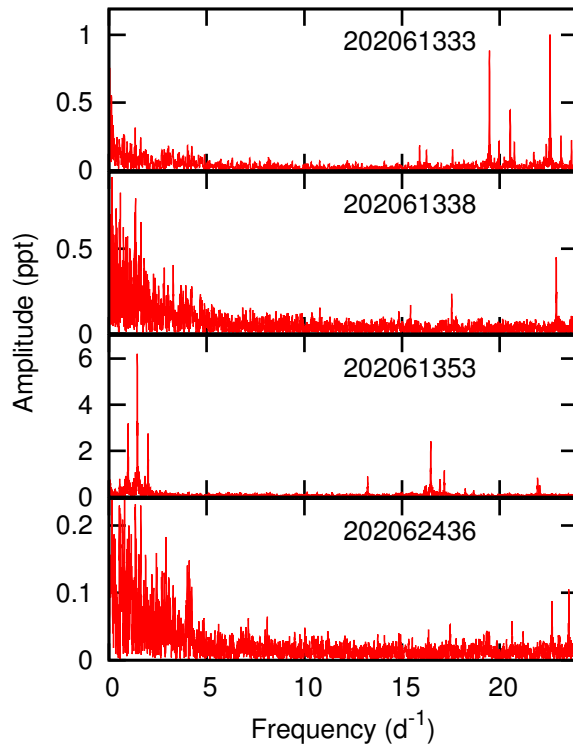


Figure 11. Periodograms of Am δ Sct stars observed in the K2 Campaign 0.

perature of EPIC 202062436 was obtained through our own analysis of the multicolour photometry.

EPIC 202061353 is a known δ Sct star from *SuperWasp* photometry (Smalley et al. 2011). This is confirmed by the K2 data (Fig. 11). The main feature is a triplet of low-frequency peaks at 1.452 , 0.980 and 2.000 d^{-1} which are not quite equally spaced.

The periodogram of EPIC 202059291 shows only two significant peaks. Considering the very low amplitude, the variability is best understood as rotational modulation with period $P = 2.984 \text{ d}$, but it could also be interpreted as a contact binary. One of us (GC) obtained a single spectrum of this star which appears to be a double-lined spectroscopic binary. It can probably be ruled out as an Am star. The periodogram and phased light curve is shown in Fig. 12.

The light curve of EPIC 202062447 (Fig. 13) shows that it is a γ Dor of the ASYM type (Balona et al. 2011b). The periodogram shows dominant periods of 0.912 d and 0.773 d .

The field of EPIC 202062450 contains two stars of almost equal brightness separated by 5 arcsec . The brighter star, FI Ori, is a detached eclipsing binary with $P = 4.4478 \text{ d}$ and spectral type K0III/IV (Halbedel 1985). The eclipses are very easily seen in the K2 combined light of the two stars. The fainter star, HD 256320 B has a spectral type kA5hA8mF5 (Halbedel 1985). We constructed an aperture which only included this star, but could not find any evidence of periodic variation with an amplitude exceeding 5 ppt .

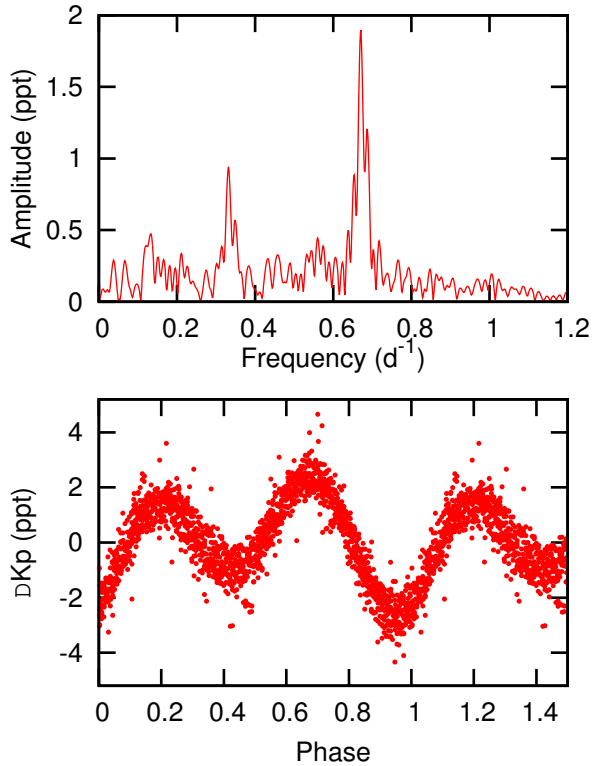


Figure 12. Top panel: periodogram of EPIC 202059291. Light curve phased with period $P = 2.984$ d.

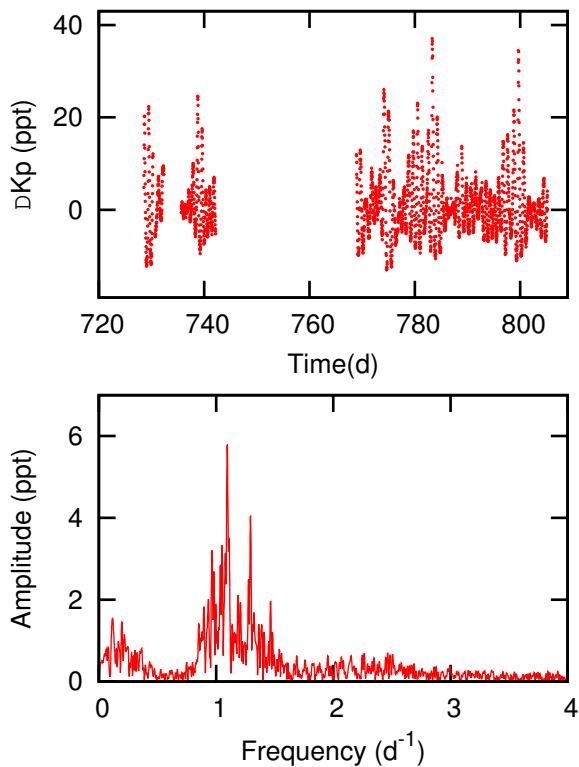


Figure 13. Top panel: light curve of EPIC 202062447 showing typical asymmetric light curve of a γ Dor star of type ASYM. The bottom panel shows the periodogram.

6 DISCUSSION AND CONCLUSION

It is evident from Table 1 that most Am stars in the *Kepler* field exhibit rotational modulation. An idea of the spot size may be gained from the light amplitude of the modulation shown in Table 1. There are only 10 Am stars in the *Kepler* field known to be rotational variables and the amplitude range is large. The mean amplitude is 93 ± 25 ppm. The mean rotational amplitude from 875 A stars in Balona (2013) is 541 ± 86 ppm. This seems to suggest that, in general, spots on Am stars are smaller than on normal A stars, but it is not possible to draw a definite conclusion owing to the small sample.

One or more flares appear to be seen in two confirmed Am stars, KIC 8703413 and KIC 9117875. The relatively large flare intensities imply that if the origin of the flare is a cool companion, the flare must be about two orders of magnitude more intense than on an isolated cool star owing to the much larger luminosity of the Am star. While this is not impossible, it seems very improbable. It is clear from a study of a much larger number of A stars that the flares cannot all be attributed to a cool companion (Balona 2012, 2013).

The presence of starspots and flares on Am stars suggests that Am stars may have significant magnetic fields similar in strength to normal A stars. The magnetic fields in both Am and normal A stars are sufficiently intense to form starspots and flares. Hence the idea that the superficial metal enrichment in Am stars is a result of the effects of diffusion and gravitational settling in the absence of a magnetic field may need to be revised. Furthermore, the relative number of pulsating Am stars is similar to the relative number of δ Sct stars among the A star population. Am stars which are δ Sct variables occupy the same region of the instability strip as normal δ Sct stars (Smalley et al. 2011). All these observations are contrary to the view that Am stars are formed by diffusion of elements in the absence of a magnetic field and that δ Sct pulsation in Am stars only occurs near the red edge of the instability strip. Given these facts, one has to conclude either that the diffusion model for Am stars needs to be revised or that it is incorrect.

Thermohaline convection takes place when a layer of enhanced metal abundance is formed above layers of lighter mean molecular weight. This happens in the case of accretion of predominantly metal-rich material (Vauclair 2004), and also when such a layer is formed due to atomic diffusion. This important effect has only recently been studied. Théado et al. (2009) finds that accumulation of heavy elements due to atomic diffusion is attenuated when thermohaline mixing is taken into account, though not completely suppressed. The inclusion of the thermohaline instability in A-star models needs to be more fully investigated to see whether this can reconcile the diffusion model of Am stars with observations.

The presence of pulsations in Am stars is only one symptom of a more general problem which has been encountered since the advent of *Kepler* photometry. For example, it is not understood why less than half of stars in the δ Sct instability strip pulsate (Balona & Dziembowski 2011), or why low-frequency pulsations are a general feature of all δ Sct stars (Balona 2014b). Further exploration of pulsational driving needs to be undertaken. For example, coherent pulsations

may be driven by turbulent pressure in the hydrogen ionization zone (Antoci 2014).

It is well established that stars hosting planets are metal rich, but the reason for such metal enhancement is still a subject for debate. The enhancement may be primordial, the result of accretion or both. The argument against an accretion origin is related to the mass of the outer convective zones, which varies by more than one order of magnitude among the considered stars, while the observed over-abundances of metals are about the same. Vauclair (2004) found that thermohaline convection mixes the accreted matter and leaves only a very small μ -gradient at the end of the mixing process. The remaining μ gradient is too small to account for the observed overmetallicity (see also Théado & Vauclair (2012)). It should be noted, however, that all these calculations are confined to solar-type stars. The effect of thermohaline convection on intermediate mass A stars has not yet been determined.

Considering the problems encountered by standard diffusion theory in explaining the properties of Am stars, it may be appropriate to again consider the possibility that the Am phenomenon may be a combination of diffusion with accretion. For example, Böhm-Vitense (2006) has argued that accretion of interstellar material by A stars with tangled magnetic fields, which are weaker than those in peculiar A (Ap) stars, has the best chance of explaining the main characteristics of the peculiar heavy-element abundances in Am star photospheres. Another look at accretion of close-in planets should also be made. We know, for example, that accretion of comet-sized bodies is very likely occurring in the A6V star β Pic which is surrounded by a debris disk (Beust et al. 1996). There is no reason to suppose that this star is unique and we can expect infalling material, even of planets, to occur. As Pinsonneault et al. (2001) has pointed out, the mass of the outer convective zone decreases rapidly for hot stars, being very thin in A stars. Therefore one may expect infalling material, mixed only in the thin outer convective zone, to have a substantial effect on the observed metallicity. For example, the mass above the base of the HeII convective zone in a typical mid-A star is less than the mass of the Earth. Since the original fraction of metals in the star is only about 2 percent of the mass of the zone, even a body much smaller than the Earth could increase the apparent metal abundance by a factor of two or more. It would be surprising if no such impacts ever occurred. Therefore one should not be surprised by the peculiar metal abundances in some A stars.

The chemically peculiar λ Boo stars have an unusually low superficial abundance of iron peak elements. It is thought that this may be a result of accretion of interstellar material as the star travels through a diffuse interstellar cloud (Kamp et al. 2008). However, the abundance pattern in λ Boo stars is very different from Am stars. This may reflect differences in abundance between the metal-poor interstellar medium and the metal-rich composition of infalling small planetary bodies.

ACKNOWLEDGMENTS

This paper includes data collected by the *Kepler* mission. Funding for the *Kepler* mission is provided by the NASA

Science Mission directorate. The authors wish to thank the *Kepler* team for their generosity in allowing the data to be released and for their outstanding efforts which have made these results possible.

Much of the data presented in this paper were obtained from the Mikulski Archive for Space Telescopes (MAST). STScI is operated by the Association of Universities for Research in Astronomy, Inc., under NASA contract NAS5-26555. Support for MAST for non-HST data is provided by the NASA Office of Space Science via grant NNX09AF08G and by other grants and contracts.

LAB wishes to thank the South African Astronomical Observatory and the National Research Foundation for financial support.

REFERENCES

- Abt H. A., 1967, in *Magnetic and Related Stars*, Cameron R. C., ed., p. 173
 —, 1981, *ApJS*, 45, 437
 —, 1984, *ApJ*, 285, 247
 Abt H. A., Levy S. G., 1985, *ApJS*, 59, 229
 Ammons S. M., Robinson S. E., Strader J., Laughlin G., Fischer D., Wolf A., 2006, *ApJ*, 638, 1004
 Antoci V., 2014, in *IAU Symposium*, Vol. 301, IAU Symposium, Guzik J. A., Chaplin W. J., Handler G., Pigulski A., eds., pp. 333–340
 Antoci V., Handler G., Campante T. L., Thygesen A. O., Moya A., Kallinger T., Stello D., Grigahcène A., Kjeldsen H., Bedding T. R., Lüftinger T., Christensen-Dalsgaard J., Catanzaro G., Frasca A., De Cat P., Uytterhoeven K., Bruntt H., Houdek G., Kurtz D. W., Lenz P., Kaiser A., van Cleve J., Allen C., Clarke B. D., 2011, *Nature*, 477, 570
 Aurière M., Wade G. A., Lignières F., Hui-Bon-Hoa A., Landstreet J. D., Iliev I. K., Donati J.-F., Petit P., Roudier T., Théado S., 2010, *A&A*, 523, A40
 Balona L. A., 2012, *MNRAS*, 423, 3420
 —, 2013, *MNRAS*, 431, 2240
 —, 2014a, *MNRAS*, 443, 1946
 —, 2014b, *MNRAS*, 437, 1476
 —, 2014c, *MNRAS*, 441, 3543
 Balona L. A., Cunha M. S., Kurtz D. W., Brandão I. M., Gruberbauer M., Saio H., Östensen R., Elkin V. G., Borucki W. J., Christensen-Dalsgaard J., Kjeldsen H., Koch D. G., Bryson S. T., 2011a, *MNRAS*, 410, 517
 Balona L. A., Dziembowski W. A., 2011, *MNRAS*, 417, 591
 Balona L. A., Guzik J. A., Uytterhoeven K., Smith J. C., Tenenbaum P., Twicken J. D., 2011b, *MNRAS*, 415, 3531
 Balona L. A., Ripepi V., Catanzaro G., Kurtz D. W., Smalley B., De Cat P., Eyer L., Grigahcène A., Lecia S., Southworth J., Uytterhoeven K., van Winckel H., Christensen-Dalsgaard J., Kjeldsen H., Caldwell D. A., van Cleve J., Girouard F. R., 2011c, *MNRAS*, 414, 792
 Batten A. H., Fletcher J. M., Mann P. J., 1978, *Publications of the Dominion Astrophysical Observatory Victoria*, 15, 121
 Bertaud C., 1960, *Journal des Observateurs*, 43, 129
 Beust H., Lagrange A.-M., Plazy F., Mouillet D., 1996, *A&A*, 310, 181
 Böhm-Vitense E., 2006, *PASP*, 118, 419

- Brown T. M., Latham D. W., Everett M. E., Esquerdo G. A., 2011, *AJ*, 142, 112
- Carquillat J.-M., Prieur J.-L., 2007, *MNRAS*, 380, 1064
- Catanzaro G., Balona L. A., 2012, *MNRAS*, 421, 1222
- Catanzaro G., Ripepi V., 2014, *MNRAS*, 441, 1669
- Catanzaro G., Ripepi V., Bernabei S., Marconi M., Balona L., Kurtz D. W., Smalley B., Borucki W. J., Bruntt H., Christensen-Dalsgaard J., Grigahcène A., Kjeldsen H., Koch D. G., Monteiro M. J. P. F. G., Suárez J. C., Szabó R., Uytterhoeven K., 2011, *MNRAS*, 411, 1167
- Catanzaro G., Ripepi V., Leone F., Frasca A., Busá I., Giarrusso M., Biazzo K., Munari M., Scuderi S., 2015, *MNRAS*, in preparation
- Fehrenbach C., Duflo M., Mannone C., Burnage R., Genty V., 1997, *A&AS*, 124, 255
- Floquet M., 1970, *A&AS*, 1, 1
- , 1975, *A&AS*, 21, 25
- Gilliland R. L., Jenkins J. M., Borucki W. J., Bryson S. T., Caldwell D. A., Clarke B. D., Dotson J. L., Haas M. R., Hall J., Klaus T., Koch D., McCauliff S., Quintana E. V., Twicken J. D., van Cleve J. E., 2010, *ApJ*, 713, L160
- Halbedel E. M., 1985, *PASP*, 97, 434
- Jenkins J. M., Caldwell D. A., Chandrasekaran H., Twicken J. D., Bryson S. T., Quintana E. V., Clarke B. D., Li J., Allen C., Tenenbaum P., Wu H., Klaus T. C., Middour C. K., Cote M. T., McCauliff S., Girouard F. R., Gunter J. P., Wohler B., Sommers J., Hall J. R., Uddin A. K., Wu M. S., Bhavsar P. A., Van Cleve J., Pletcher D. L., Dotson J. A., Haas M. R., Gilliland R. L., Koch D. G., Borucki W. J., 2010a, *ApJ*, 713, L87
- Jenkins J. M., Caldwell D. A., Chandrasekaran H., Twicken J. D., Bryson S. T., Quintana E. V., Clarke B. D., Li J., Allen C., Tenenbaum P., Wu H., Klaus T. C., Van Cleve J., Dotson J. A., Haas M. R., Gilliland R. L., Koch D. G., Borucki W. J., 2010b, *ApJ*, 713, L120
- Kamp I., Martínez-Galarza J. R., Paunzen E., Su K. Y. L., Gáspár A., Rieke G. H., 2008, *Contributions of the Astronomical Observatory Skalnaté Pleso*, 38, 147
- Luyten W. J., 1936, *ApJ*, 84, 85
- Macrae D. A., 1952, *ApJ*, 116, 592
- McCuskey S. W., 1959, *ApJS*, 4, 23
- , 1967, *AJ*, 72, 1199
- Mendoza E. E., 1974, *RMxAA*, 1, 175
- Murphy S. J., Bedding T. R., Shibahashi H., Kurtz D. W., Kjeldsen H., 2014, *MNRAS*, 441, 2515
- Murphy S. J., Grigahcène A., Niemczura E., Kurtz D. W., Uytterhoeven K., 2012, *MNRAS*, 427, 1418
- Paunzen E., Wraight K. T., Fossati L., Netopil M., White G. J., Bewsher D., 2013, *MNRAS*, 429, 119
- Pinsonneault M. H., DePoy D. L., Coffee M., 2001, *ApJ*, 556, L59
- Prša A., Batalha N., Slawson R. W., Doyle L. R., Welsh W. F., Orosz J. A., Seager S., Rucker M., Mjaseth K., Engle S. G., Conroy K., Jenkins J., Caldwell D., Koch D., Borucki W., 2011, *AJ*, 141, 83
- Renson P., Manfroid J., 2009, *A&A*, 498, 961
- Richer J., Michaud G., Turcotte S., 2000, *ApJ*, 529, 338
- Shibahashi H., Kurtz D. W., 2012, *MNRAS*, 422, 738
- Slawson R. W., Prša A., Welsh W. F., Orosz J. A., Rucker M., Batalha N., Doyle L. R., Engle S. G., Conroy K., Coughlin J., Gregg T. A., Fetherolf T., Short D. R., Windmiller G., Fabrycky D. C., Howell S. B., Jenkins J. M., Uddin K., Mullally F., Seader S. E., Thompson S. E., Sanderfer D. T., Borucki W., Koch D., 2011, *AJ*, 142, 160
- Smalley B., Kurtz D. W., Smith A. M. S., Fossati L., Anderson D. R., Barros S. C. C., Butters O. W., Collier Cameron A., Christian D. J., Enoch B., Faedi F., Haswell C. A., Hellier C., Holmes S., Horne K., Kane S. R., Lister T. A., Maxted P. F. L., Norton A. J., Parley N., Pollacco D., Simpson E. K., Skillen I., Southworth J., Street R. A., West R. G., Wheatley P. J., Wood P. L., 2011, *A&A*, 535, A3
- Smalley B., Southworth J., Pintado O. I., Gillon M., Holdsworth D. L., Anderson D. R., Barros S. C. C., Collier Cameron A., Delrez L., Faedi F., Haswell C. A., Hellier C., Horne K., Jehin E., Maxted P. F. L., Norton A. J., Pollacco D., Skillen I., Smith A. M. S., West R. G., Wheatley P. J., 2014, *A&A*, 564, A69
- Smith J. C., Stumpe M. C., Van Cleve J. E., Jenkins J. M., Barclay T. S., Fanelli M. N., Girouard F. R., Kolodziejczak J. J., McCauliff S. D., Morris R. L., Twicken J. D., 2012, *PASP*, 124, 1000
- Stumpe M. C., Smith J. C., Van Cleve J. E., Twicken J. D., Barclay T. S., Fanelli M. N., Girouard F. R., Jenkins J. M., Kolodziejczak J. J., McCauliff S. D., Morris R. L., 2012, *PASP*, 124, 985
- Talon S., Richard O., Michaud G., 2006, *ApJ*, 645, 634
- Théado S., Vauclair S., 2012, *ApJ*, 744, 123
- Théado S., Vauclair S., Alecian G., Le Blanc F., 2009, *ApJ*, 704, 1262
- Turcotte S., Richer J., Michaud G., Christensen-Dalsgaard J., 2000, *A&A*, 360, 603
- Uytterhoeven K., Moya A., Grigahcène A., Guzik J. A., Gutiérrez-Soto J., Smalley B., Handler G., Balona L. A., Niemczura E., Fox Machado L., Benatti S., Chapellier E., Tkachenko A., Szabó R., Suárez J. C., Ripepi V., Pascual J., Mathias P., Martín-Ruiz S., Lehmann H., Jackiewicz J., Hekker S., Gruberbauer M., García R. A., Dumusque X., Díaz-Fraile D., Bradley P., Antoci V., Roth M., Leroy B., Murphy S. J., De Cat P., Cuypers J., Kjeldsen H., Christensen-Dalsgaard J., Breger M., Pigulski A., Kiss L. L., Still M., Thompson S. E., van Cleve J., 2011, *A&A*, 534, A125
- Vauclair S., 2004, *ApJ*, 605, 874
- Vauclair S., Théado S., 2012, *ApJ*, 753, 49
- Walkowicz L. M., Basri G., Batalha N., Gilliland R. L., Jenkins J., Borucki W. J., Koch D., Caldwell D., Dupree A. K., Latham D. W., Meibom S., Howell S., Brown T. M., Bryson S., 2011, *AJ*, 141, 50
- Wraight K. T., Fossati L., Netopil M., Paunzen E., Rode-Paunzen M., Bewsher D., Norton A. J., White G. J., 2012, *MNRAS*, 420, 757